Available online at www.sciencedirect.com
ScienceDirect
Journal of Chromatography B, 860 (2007) 218–226
JOURNAL OF CHROMATOGRAPHY B
www.elsevier.com/locate/chromb

Structure elucidation of metabolites of gambogic acid *in vivo* in rat bile by high-performance liquid chromatography–mass spectrometry and high-performance liquid chromatography–nuclear magnetic resonance

Feng Feng [a], Wenyuan Liu [b,*], Yinghong Wang [c], Qinglong Guo [d], Qidong You [e,*]

[a] *Department of Phytochemistry, China Pharmaceutical University, Nanjing 210009, China*
[b] *Department of Pharmaceutical Analysis, China Pharmaceutical University, Nanjing 210009, China*
[c] *Institute of Materia Medica, Chinese Academy of Medical Science & Peking Union Medical College, Beijing 100050, China*
[d] *Department of Physiology, China Pharmaceutical University, Nanjing 210009, China*
[e] *Department of Medicinal Chemistry, China Pharmaceutical University, Nanjing 210009, China*

Received 21 April 2007; accepted 23 October 2007
Available online 1 November 2007

Abstract

Gambogic acid (GBA), the main component of Gamboge, possesses significant anti-tumour activity. Due to its structural complexity, little is known about GBA metabolism. Here, we investigate the metabolism of GBA *in vivo* in rat bile. Identification of the metabolites formed was elucidated using high-performance liquid chromatography (HPLC) with UV–vis detection, HPLC/ion trap electrospray ionization-mass spectrometry, as well as HPLC/nuclear magnetic resonance. Four main metabolites were determined. Two phase I metabolites, 10-hydroxygambogic acid and 9,10-epoxygambogic acid, were oxides on the 9,10-olefinic bond of GBA. The others phase II metabolites, were 9,10-epoxygambogic acid-30-*O*-glucuronide and 10-hydroxylgambogic acid-30-*O*-glucuronide.

Keywords: Gambogic acid; Metabolites; Structural determination; 10-Hydroxygambogic acid; 9,10-Epoxygambogic acid

1. Introduction

Gamboge, the juice that is secreted from the trunk of *Garcinia* L. Planch (e.g. *Garcinia hanburyi* Hook. and *Garcinia morella* Gesv.), is used in traditional Chinese medicine for detoxification, maintaining hemostasis, and as an anthelmintic [1]. Gambogic acid (GBA), the primary component of Gamboge, is a prenylated xanthonoid that has the bridged structural moiety of tricyclo-4-oxa[4.3.1.0]decan-2-one. It has been reported that GBA is cytotoxic against various cancer cell lines and is a potent inducer of apoptosis. Previous studies have shown that GBA inhibited the growth of cultured human hepatoma SMMC-7721 cells, possibly by inhibiting telomerase activity [2]. Inhibition of the growth of SPA-A1 cells and its tumor xenografts by GBA has also been reported. After treatment with GBA for a period of time, both the telomerase activity and the expression of hTERT mRNA in the tumor cells were significantly inhibited. The inhibitory mechanism of GBA in SPA-A1 cells may be due to the modification of hTERT mRNA expression that leads to the down-regulation of telomerase activity [3]. Thus, GBA is an effective telomerase inhibitor and displays potent anticancer activity both *in vitro* and *in vivo*. Moreover, GBA has been shown to induce apoptosis in a cell cycle independent manner. Studies examining the selective induction of apoptosis by GBA on MGC-803 cells revealed that activation of the *bax* gene and suppression of the *bcl-2* gene may contribute to the apoptosis mechanism [4]. Another study suggested that GBA binds to the transferring receptor inducing a unique signal that leads to rapid apoptosis of tumor cells [5].

Pharmacokinetic studies of GBA in rats showed that, following i.v. administration, GBA was mainly distributed in the

Abbreviations: FID, free induction decays; GBA, gambogic acid; HPLC, high-performance liquid chromatography; LC/ESI(−)-MS, liquid chromatography/negative ion electrospray ionization-mass spectra; LC–MS, liquid chromatography–mass spectrometry; MS, mass spectrometry; NMR, nuclear magnetic resonance; RP-HPLC, reverse phase high-performance liquid chromatography; SPE, solid phase extraction; UV, ultraviolet; IR, infra-red.

* Corresponding authors.
E-mail address: liuwenyuan8506@163.com (W. Liu).

1570-0232/$ – see front matter © 2007 Elsevier B.V. All rights reserved.
doi:10.1016/j.jchromb.2007.10.037

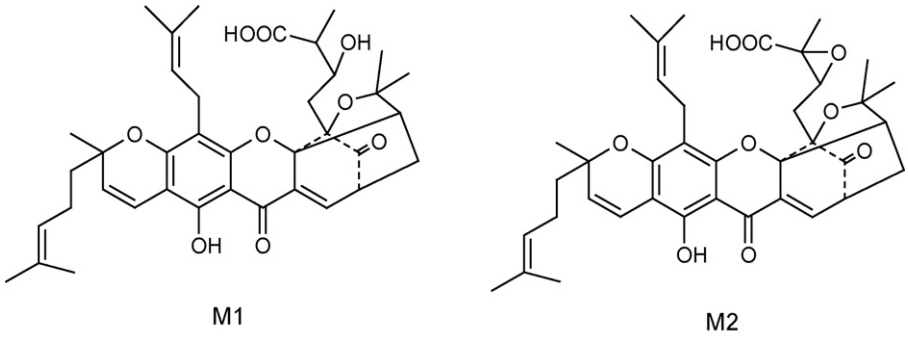

Fig. 1. The structures of M1 and M2.

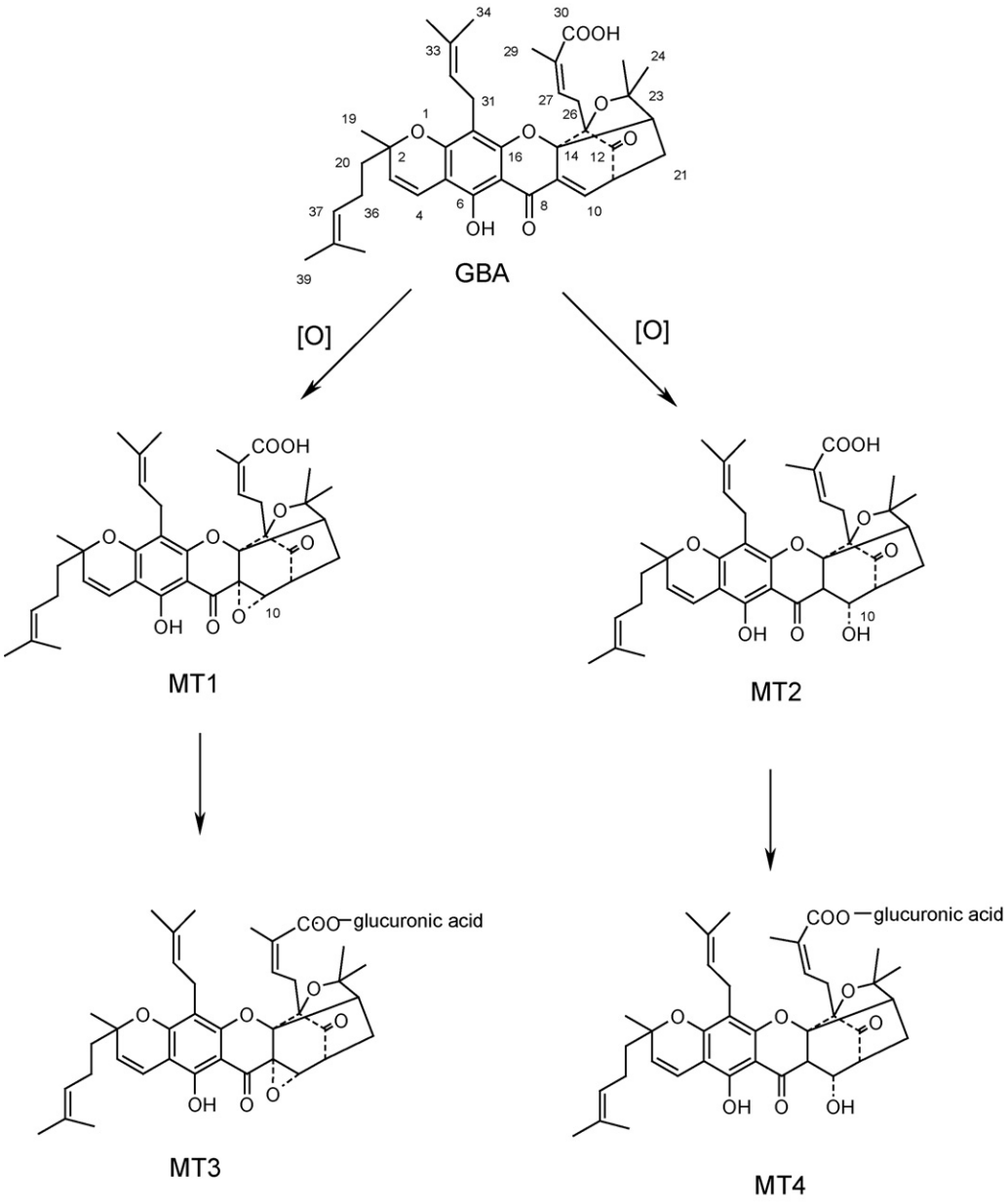

Fig. 2. The proposed metabolic pathway of GBA *in vivo* in rat bile.

organs such as in the liver, lung, spleen, kidney, stomach, intestine and heart. GBA was mainly excreted through bile with approximately 36.5% being excreted within 16 h. In addition, only traces of GBA appeared in the feces, and no GBA was detected in the urine [6].

Rat liver microsomes have been used previously to study the effects of selective CYP450 inhibitors on the metabolism of GBA [7]. GBA was shown to rapidly metabolize into two phase I metabolites, M1 and M2 (Fig. 1). However, due to the structural complexity of GBA, the liquid chromatography-mass spectrometry (LC–MS), ultraviolet (UV) and mass spectrometry (MS) data obtained in that report was not sufficient to determine the location of the hydroxyl and epoxy groups. Indeed, our findings indicate that the previously reported structural identification of these metabolites was incorrect. Here, we use reverse phase high-performance liquid chromatography (RP-HPLC) with UV and ion-trap mass spectrometry on the bile extracted from GBA-treated rats to detect four main metabolites of GBA. The extracted bile was separated by RP-HPLC followed by nuclear magnetic resonance (NMR) analysis. The structures of the four metabolites were determined by the integrative analysis of UV, LC–MS and LC–NMR data as 10-hydoxygambogic acid, 9,10-epoxygambogic acid, and their respective glucuronid conjugates (Fig. 2).

2. Experimental

2.1. Chemicals and reagents

GBA was prepared by the Department of Phytochemistry, China Pharmaceutical University (Nanjing, China). HPLC/UV analysis indicated that the preparation was over 98% pure. Its structure was identified by comprehensive analysis of high-resolution mass spectroscopy, UV, IR, 1D and 2D NMR spectra. All chemicals and solvents were of analytical or HPLC grade. Acetonitrile and methanol were obtained from Merck (Darmstadt, Germany). Water was prepared using a Milli-Q water purification system (Millipore Corporation, Billerica, MA, USA). The sample was prepared by dissolving arginine (22 mg) in water (2.0 ml), then adding GBA (20 mg) and stirring until the GBA had dissolved completely. The solution was filtered with a syringe filter to ensure that its final concentration was 10 mg/ml GBA. The sample was stored at 4 °C for no more than 4 h.

2.2. Animal dosing and sample collection

Ten male Sprague–Dawley rats (weighing 300–400 g) were fasted for 16–22 h with free access to water. A cannula was implanted for the bile collection. The blank bile was collected before administration. The rats were under ether anesthesia for the entire duration of the surgery. After recovery from the surgery, the pre-prepared drug solution was injected into the vena caudalis at a dose of 6.0 mg/kg. The bile was collected on ice for 12 h. The rats were given water occasionally during the course of bile collection.

2.3. HPLC analysis of biliary metabolites

HPLC analysis was carried out with a system that consisted of a Shimadzu 10AD pump and a Shimadzu 10A UV–vis detector (Kyoto, Japan). A MetaChem Technologies (Lake Forest, CA, USA) Inertsil C18 5-μm column (4.6 mm × 150 mm) was used. The mobile phase was 85% CH_3OH in water at a flow rate of 1.0 ml/min, and the wavelength of the UV detector was 280 nm. The chromatography was recorded and analyzed by the N2000 workstation (Hangzhou, China). Blank and administrated bile samples (200 μl) were acidified with 20 μl 0.1% H_3PO_4 solution, and extracted with 500 μl of EtOAc. The EtOAc layer was separated and the supernatant was evaporated to dryness under a stream of N_2 at 45 °C. The residue was redissolved in 200 μl of the LC mobile phase and centrifuged at 5000 rpm (Beckman Coulter Microfuge 18 centrifuge) for 3 min before analysis. Twenty microliters of sample were analyzed.

2.4. LC/MS analysis of biliary metabolites

Liquid chromatography/negative ion electrospray ionization-mass spectra (LC/ESI(−)-MS) of GBA and its metabolites were acquired on a HPLC system (HP1100; Agilent Technologies Inc., CA, USA) coupled with the Agilent LC/MSD ion trap mass spectrometer (Agilent Technologies Inc.). The instrument was operated in the negative electrospray ionization mode. The capillary voltage was fixed at 16 V, and its temperature was maintained at 200 °C. The spray voltage was set at 4.25 kV. The HPLC fluid was nebulized using N_2 as both the sheath gas at a flow rate of 0.75 l/min, and the auxiliary gas at a flow rate of 0.15 l/min. The MS/MS spectra were produced by collision-induced dissociation of the selected precursor ions with helium present in the mass analysis. The relative collision energy was set at 30–40%. Data were collected and analyzed using the LC/MSD ChemStation software (Agilent Technologies Inc.).

2.5. LC/NMR analysis of biliary metabolites

LC/NMR spectra were obtained on a HPLC system consisting of a ProStar 230 ternary solvent delivery module and a ProStar 330 photodiode array detector (Palo Alto, CA, USA) connected to a Varian INOVA 500 MHz High Resolution NMR Spectrometer that was equipped with a $^1H\{^{13}C\}$ pulsed field gradient LC–NMR flow-probe with a 60 μl flow-cell. ^1H-NMR spectra were obtained in the stopped-flow mode at 500.13 MHz. Varian WET solvent suppression and related sequences were used to suppress the residual water peaks. Free induction decays (FID) were collected with 16 K data points, a spectral width of 7500 Hz, a 1.5 s acquisition time, and a 1 s pulse delay. A total of 256 transients were acquired to obtain the ^1H NMR data. Prior to Fourier transformation, an exponential apodisation function was applied to the FID corresponding to a line broadening of 1.0 Hz. Administrated bile samples (500 μl) were acidified with 100 μl 0.1% H_3PO_4 solution, and extracted with 2 ml of EtOAc. The EtOAc layer was concentrated at 50 °C. Residue was redissolved in 20 μl methanol and centrifuged at 5000 rpm (Beckman Coul-

ter Microfuge 18 centrifuge) for 3 min before analysis. Twenty microliters of sample were analyzed.

3. Results and discussion

HPLC analysis revealed the presence of four main metabolites of GBA (Fig. 3). Compared to the chromatograms of GBA that showed a peak at 21.5 min, the biliary samples showed four main metabolites at 8.7 (MT4), 8.2 (MT3), 18.0 (MT2), and 19.1 (MT1) min. The UV spectra of all metabolites (Fig. 4B–E) were different from that of GBA (Fig. 4A), indicating that they had different conjugate systems to GBA. However, it was difficult to determine the structural differences between GBA and its metabolites because GBA has several different conjugate systems including benzopyran, benzopyrone and α,β-unsaturated carbonyl units [1]. In addition, the structure of the GBA metabolites could not be determined from the MS data. The MS data showed that MT1 (Fig. 5A) and MT2 (Fig. 5B) were the oxide and hydrate of GBA, respectively. However, GBA has several active olefinic bonds that could potentially be oxidized.

LC/NMR analysis provided more information about the structure of the metabolites. Because the content of MT1 and MT2 was relatively low in the sample, and nondeuterated mobile phase was applied at the first 10 min, the solvent suppression and phasing in the high field region was bad. But it is possible to solve the structures of metabolites based on the signals on the downfield regions. The stop-flow LC–^{1}H NMR spectra of MT1, MT2 and GBA (Fig. 6) show more detailed information about the olefinic protons. On the basis of these data, MT1 and MT2 were identified as the oxides of the 9,10-double bond of GBA. The phase II metabolites, MT3 and MT4, were identified as glucuronide conjugates of MT1 and MT2, respectively. The location of the glucuronic acid was presumed by the comparison of several GBA derivates (Fig. 7). The structures of these metabolites are shown in Fig. 2.

3.1. Structural determination of MT1 (9,10-epoxygambogic acid)

The UV spectrum (Fig. 4B) showed the maximum absorptions at 274(sh), 285 and 335 nm. These were different from the

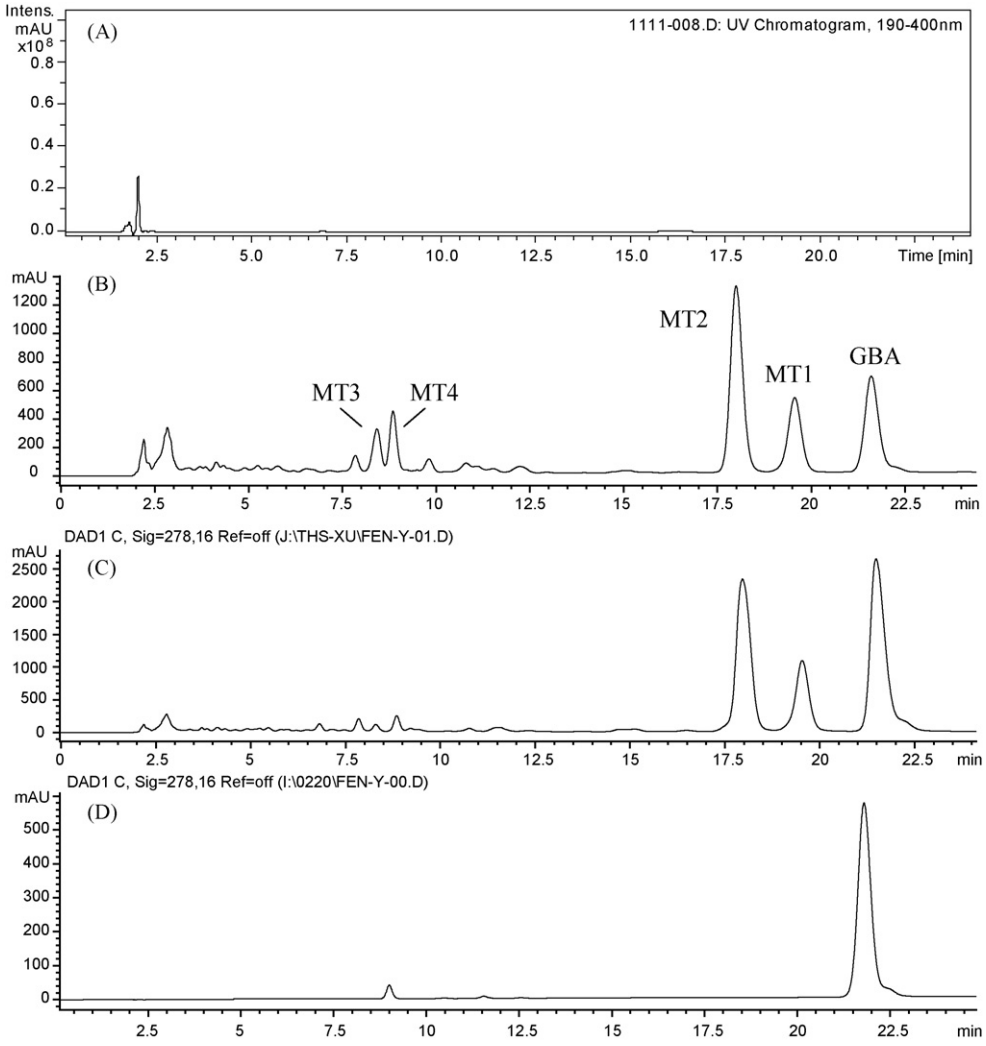

Fig. 3. Representative HPLC–UV chromatography of: (A) blank biliary; (B) bile collected 0–4 h from a male rat that had received a single dose of GBA intravenously in a tail vein with 6 mg/kg of GBA; (C) bile ample hydrolyzed by glucuronidase; (D) GBA.

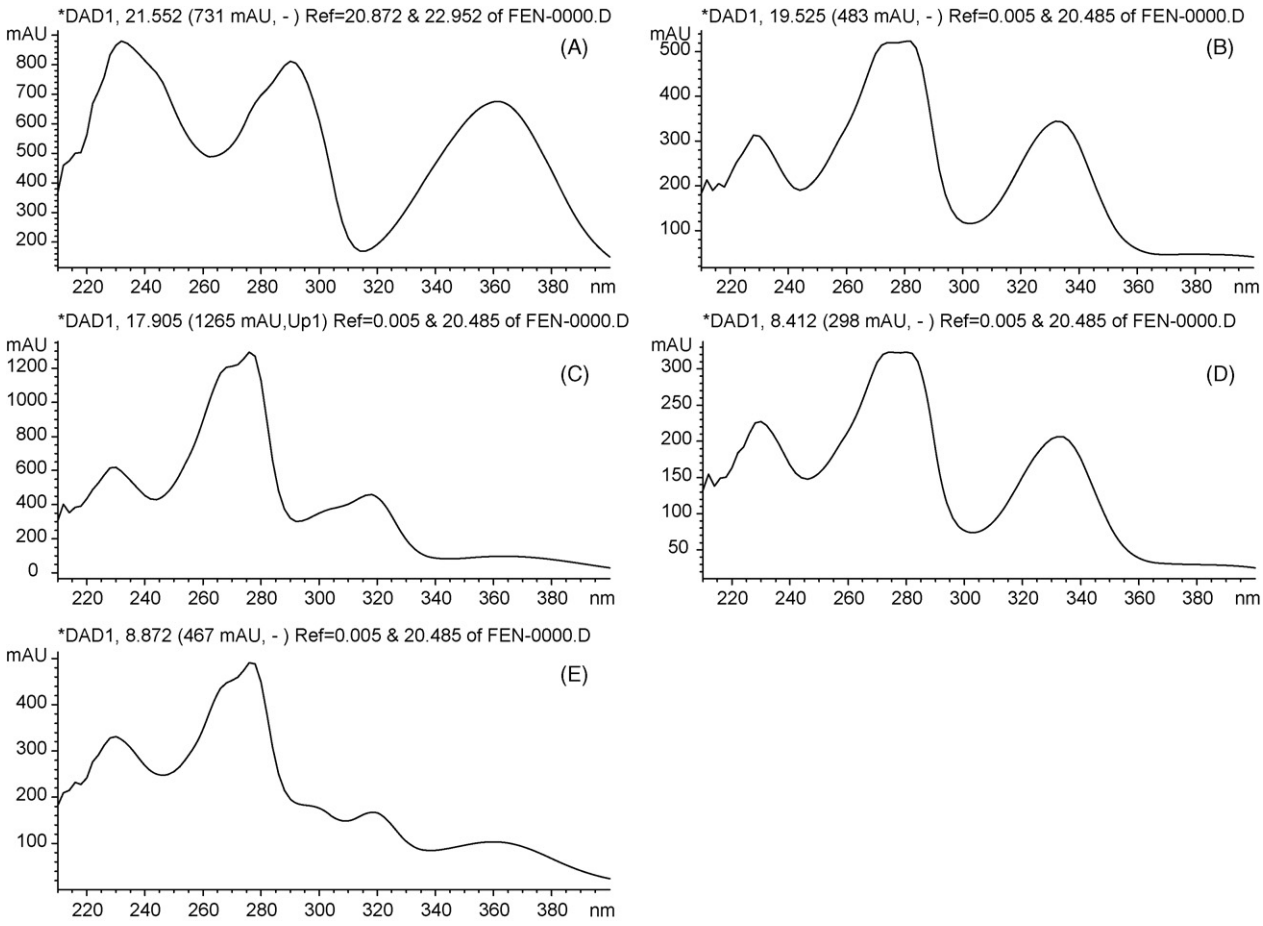

Fig. 4. UV spectra of: (A) GBA; (B) MT1; (C) MT2; (D) MT3; (E) MT4.

UV spectrum of GBA (Fig. 4A), which has a maximum absorption at 360 nm. LC–MS (Fig. 5B) showed that the M–H peak of MT1 at *m/z* 643, exceeded that of GBA *m/z* 16. Comparing the downfield signals of MT1 with those of GBA on the LC–^{1}H NMR spectra (Fig. 6B and C), the absence of the C-10 methenyl proton δ 7.60 (1H, d, J = 6.9 Hz) in GBA, together with the appearance of a proton geminal to an oxygenic group at δ 4.35 (1H, d, J = 5.0 Hz) in MT1, suggested that MT1 was the C10 oxide of GBA. Because only one more oxygen atom was added compared with the composition of GBA, MT1 could be assigned as 10-ketone or 9,10-epoxide of GBA. If there was a ketone at C10, the C9 should have an enolizable proton that would show an un-split singlet depending on the enolization equilibrium and consequent solvent exchange. It was inconsistent with the signal of 10-H at δ 4.35 (1H, d, J = 5.0 Hz). The observation of this signal as a doublet proved it was a 9,10-epoxide of GBA because the C10 proton only coupled with H-11. Usually the protons signal from the epoxyethane derivate appears at δ 2.5–3.6 [8], but the chemical shift of this proton in MT1 had shifted downfield to δ 4.3. This shift was because the proton was located in the middle of two carbonyls at a rigid bridged ring system, and was therefore subject to a strong deshielding effect. 9,10-Epoxygambogic acid has been synthesized by oxidizing GBA with H_2O_2 in 2 mol/l NaOH [9]. The published ^{1}H NMR data were coincident with those of MT1, especially for the H-10 signal (Table 1). Thus, we identified MT1 as 9,10-epoxygambogic acid.

Furthermore, because of the changing configuration of rings C and D, some differences in the alkene proton signals may be due to isopentene signals. The signal of H-27 in GBA (δ 5.97

Table 1
Comparison of the ^{1}H NMR data of MT1, MT2, GBA and 9,10-epoxy-gambogic acid

H	MT1	9,10-Epoxygambogic acid [9]	MT2	GBA
4	6.65 d, 10.0	6.66 d, 10.2	6.65 d, 10.0	6.65 d, 10.1
27	6.51 t, 7.0, 7.0	6.51 t, 6.9	6.52 t, 7.2, 7.2	5.97 t, 7.3, 7.3
3	5.64 d, 10.0	5.64 d, 9.9	5.55 d, 10.0	5.64 d, 10.1
32, 37	5.08 m	5.04–5.09 m, 2H	5.25 m	5.12 m, 2H
	5.02 m		5.05 m	
10	4.35 d, 5.0	4.35 d, 3.9	4.65 br.d, 4.0	7.60 d, 6.9

(1H, t, $J = 7.3$ Hz)) (Fig. 7B) moved downfield to δ 6.51 (1H, t, $J = 7.0$ Hz) in MT1 (Fig. 7C). The overlapping peak of H-32 and H-37 (δ 5.12 (2H, m)) in GBA (Fig. 7B) was separated into two multiplets and moved upfield in MT1 at δ 5.08 and 5.02 (each 1H, m), respectively (Fig. 6C).

3.2. Structural determination of MT2 (10-hydroxygambogic acid)

The UV spectrum of MT2 (Fig. 4C), which was different from that of GBA (Fig. 4A), showed maximum absorptions at

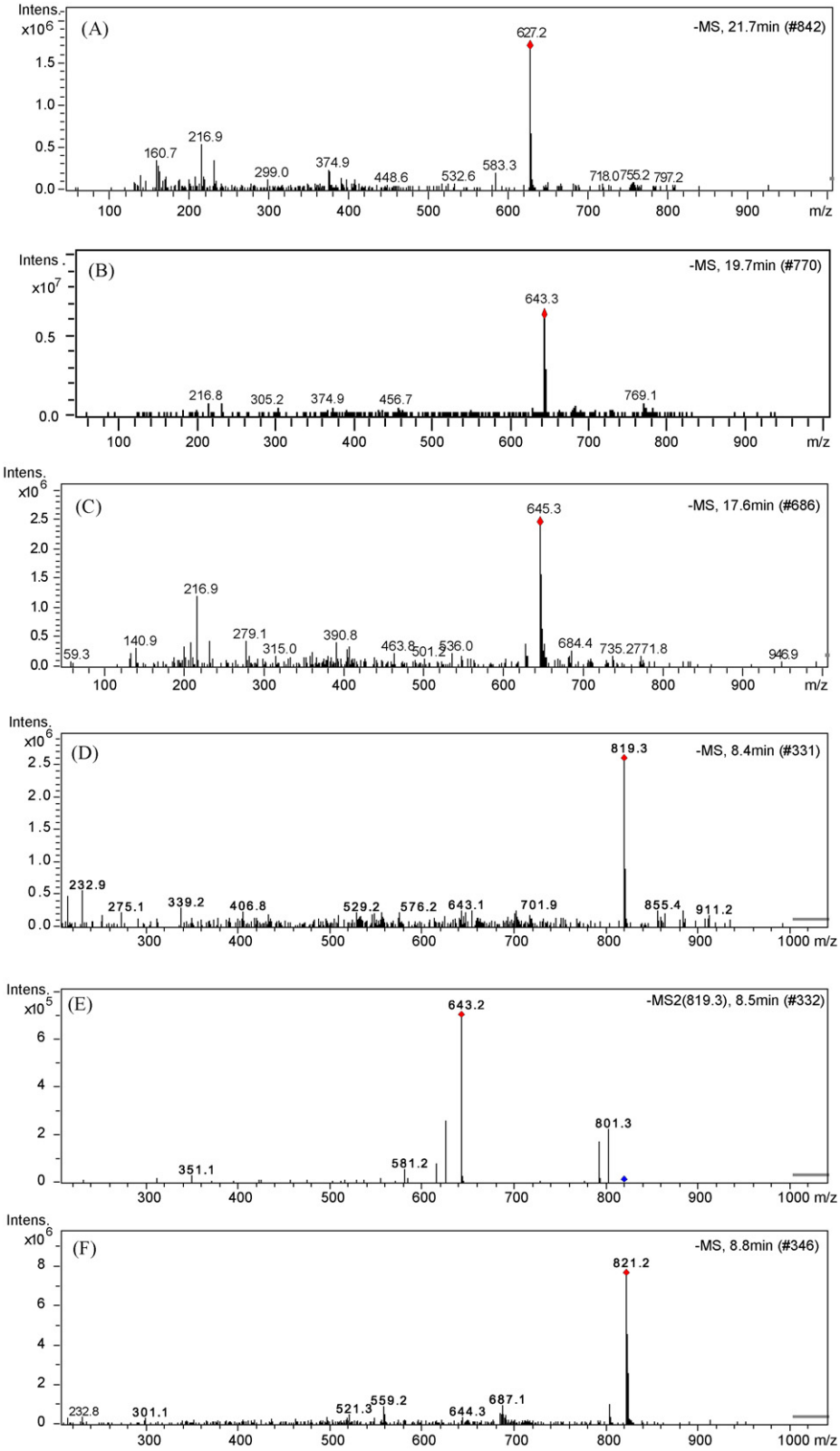

Fig. 5. Mass spectra of GBA and its metabolites obtained by ESI-MS. (A) Mass spectra of GBA; (B) mass spectra of MT1; (C) mass spectra of MT2; (D and E) MS^n spectrum of MT3; (F–H) MS^n spectrum of MT4.

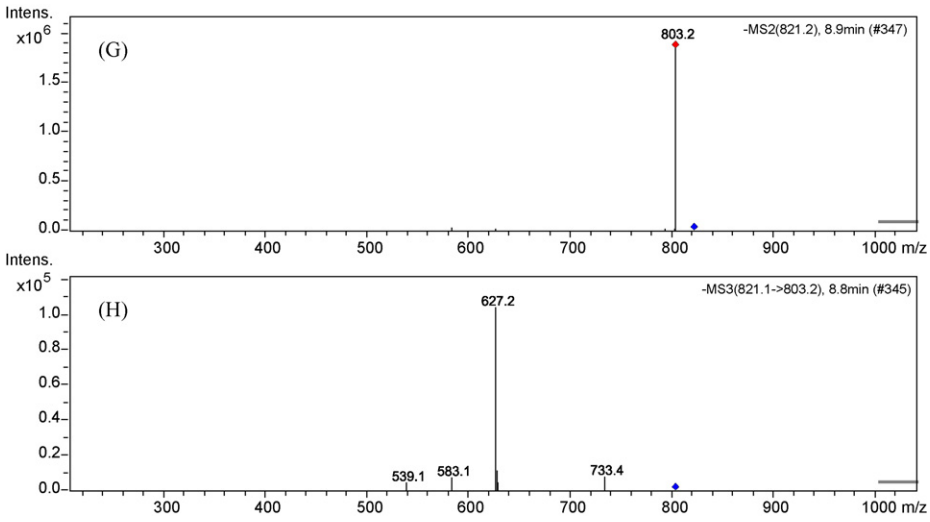

Fig. 5. (*Continued*)

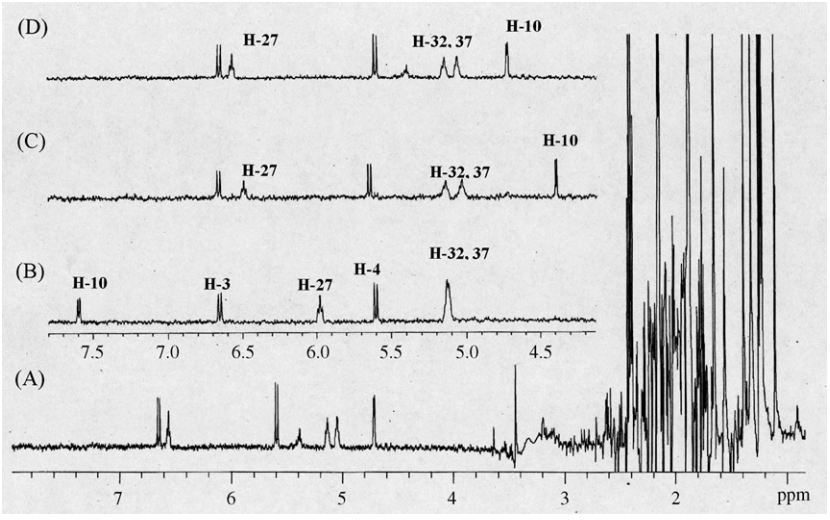

Fig. 6. Stop-flow LC–NMR spectra of the peak at t_R 18.0, 19.5 and 20.1 min, corresponding to MT2, MT1 and GBA. The spectrum was obtained after injection of 20 μl biliary samples on-column. Expansions of the signals on the downfield region were shown, and the assignment of the protons were marked. (A) Whole stop-flow spectrum of MT2; (B–D) expansions of the downfield region of the stop-flow spectrum of GBA (B), MT1 (C), and MT2 (D).

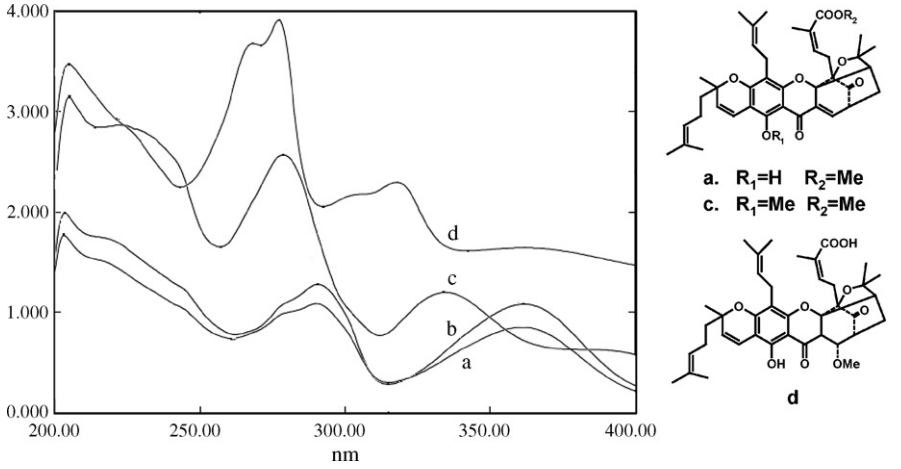

Fig. 7. The UV absorption scanning profiles for GBA's derivates (a) methyl gambogate; (b) GBA; (c) methyl-6-methoxy-gambogate; (d) 10-methoxyl gambogic acid.

267(sh), 279 and 318 nm, indicating that the 9,10-double bond might be absent. ESI-MS (Fig. 5C) showed the M–H peak of MT2 at *m/z* 645, exceeding that of GBA *m/z* 18. These data suggested that MT2 was probably the hydrate of GBA. Comparing the downfield signals of MT2 on the LC–^{1}H NMR spectrum (Fig. 6D) with that of GBA (Fig. 6B), the absence of the C-10 methenyl proton δ 7.60 (1H, d, J = 6.9 Hz) in GBA, along with the appearance of a proton geminal to an oxygenic group at δ 4.65 (1H, br.d, J = 4.0 Hz) in MT2, suggested that MT2 was the hydrate of the 9,10-olefinic bond of GBA. If the hydroxyl was at the C9 position, the C10 protons should be showed on more high-field region than δ 4.35, and the geminal coupling between C10 protons should be bigger than 4.6 Hz, it could not explain the signal atδ 4.65 (1H, br.d, J = 4.0 Hz). So the hydroxyl group should located at C-10. Furthermore, there are some differences in other olefinic protons that might be due to the presence of isopentene groups. The signal of H-27 in GBA (δ 5.97 (1H, t, J = 7.3 Hz)) moved downfield to δ 6.52 (1H, t, J = 7.2 Hz) in MT2, and the overlapping peak of H-32 and H-37 (δ 5.12 (2H, m)) in GBA were separated into two multiplets at δ 5.05 and 5.25 (each 1H, m), respectively. This was very similar to MT1 and suggested that MT2 might be 10-hydroxy-gambogic acid.

Since coupled with two asymmetric protons (H-9 and H-11), the signal of C10 proton should be a doublet and doublets as it showed in isomoreollin (1H, dd, J = 1.1, 4.6 Hz) [11]. But a broad doublet as the 10-H signal of MT2 was displayed sometimes because the coupling between H-10 and H-11 was very small, just like the reported data (1H, d, J = 4.6 Hz) of moreollic acid [11].

The structure of MT2 was determined by comparison of the NMR data between MT2 and a known compound, 10-methoxy-gambogyl piperidine, which has a signal at δ 4.33 (1H, d) corresponding to H-10 [9]. A significant downfield shift for this proton in MT2 (δ 4.65 (1H, br.d, J = 4.0 Hz)) was caused by the electronegativity of the hydroxyl group. Therefore, the structure of MT2 was identified as 10-hydroxygambogic acid.

According to the above and other reported compounds, the presence of a 9,10-double bond in GBA and its derivatives could be confirmed by the UV absorption near 360 nm [10]. The lack of this absorption on the UV spectra of MT1 and MT2 suggests that the oxidized double bond was at C-9 and C-10, but not at C-27 and C-28. On the other hand, ^{1}H NMR signals of olefinic protons are very useful for the structural determination of GBA and its derivatives [10]. A doublet of 10-olefinic protons near δ 7.6 suggests the presence of the 9,10-double bond. If this signal disappeared and was replaced by a doublet of a proton near δ 4.5, the presence of the 10-oxygenic group could be confirmed. ^{1}H NMR spectra of MT1 and MT2, showed signals near δ 4.5 and lacked those at δ 7.6, indicating that the C-10 location of the oxygenic substituents though ^{1}H NMR signals for H-9 of MT2 could not be observed because of interference by the mobile phase. Thus, the previously reported structures of two metabolites of GBA in rat liver microsomes, M1 and M2, might be incorrect due to the insufficient data obtained from LC–MS analysis alone.

3.3. Structural elucidation of MT3 and MT4

The peak of MT3 and MT4 disappeared from the HPLC–UV chromatogram after hydrolysis with β-glucuronidase (Fig. 3C), indicating that they were glucuronide conjugates. The UV spectrum of MT3 (Fig. 4D), with maximum absorptions at 274(sh), 285 and 335 nm, was almost identical to those of MT1 (Fig. 4B), suggesting that MT3 has the same structural skeleton as MT1. ESI-MS showed the pseudo-molecular ion $[M-H]^-$ at *m/z* 819 (Fig. 5D) was 176 u higher than that of MT1 (Fig. 5B), strongly suggesting that MT3 was likely to be the glucuronide conjugate of MT1. This was confirmed further by the MS/MS spectrum (Fig. 5E), which revealed that the peak of $[M-H–H_2O]^-$ (*m/z* 801) lost the glucuronyl group to give the ion segment at *m/z* 643. The latter was coincident with the pseudo-molecular ion of MT1. So MT3 was the glucuronide conjugate of 9,10-epoxygambogic acid.

The UV spectrum of MT4 (Fig. 4E) was almost the same as that of MT2. It revealed maximum absorptions at 267(sh), 279 and 318 nm, suggesting that MT4 had the same structural skeleton as MT2. ESI-MS (Fig. 5F) exhibited a pseudo-molecular ion $[M-H]^-$ at *m/z* 821, 176 u higher than that of MT2. All of these data revealed that MT4 was probably the glucuronide conjugate of MT2. It was further verified by the MS2 and MS3 spectra (Fig. 5G and H). These gave the ion at *m/z* 803, and revealed that the peak of $[M-H–H_2O]^-$ (*m/z* 803) subsequently lost the glucuronate to give the ion at *m/z* 627. This was coincident with the pseudo-molecular ion of GBA. Therefore, MT4 was the glucuronide conjugate of 10-hydroxygambogic acid.

LC–^{1}H NMR spectrum of MT3 and MT4 could not be obtained because of their low content in the metabolic sample. But we tried to determined the location of the glucuronate group by the comparison of UV spectrum of four GBA derivates (Fig. 7).

The UV spectrum of methyl gambogate (Fig. 7a) was almost the same as that of GBA (Fig. 7b), which had the UV absorption at 360 and 290 nm, whereas methyl-6-methoxy-gambogate had the UV absorptions at 334 and 279 nm (Fig. 7c). So the etherification of 6-OH could resulted in the blue shift for the UV absorption, and the esterification of 30-carboxy group didn't result in obvious shift. The UV spectra of MT3 (Fig. 4D) and MT1 (Fig. 4B) were almost the same. It proved that glucuronic acid was attached as an acyl ester in MT3. Thus, MT3 was identified as 9,10-epoxygambogic acid-30-*O*-glucuronide.

Similarly, MT4 was not an phenol glycoside too because there was no obvious shift between the UV absorptions of MT4 (Fig. 4E) and MT2 (Fig. 4C). It might be an alcoholic ether (at C-10) or an acyl ester (at C-30). The location of glucuronic acid was identified by the comparison of UV spectrum of 10-methoxyl gambogic acid (Fig. 7d) with that of MT4 (Fig. 4E) and MT2 (Fig. 4C). The UV spectrum of 10-methocyl derivate was the same as that of MT2 (Fig. 4C), a 10-hydroxyl derivate. It revealed that etherification of 10-OH didn't cause any influence on their UV spectrum. However, the UV spectrum of MT2 (Fig. 4C) had the different fine shape with MT4 (Fig. 4E) in which the absorption at 300nm was enhanced to be higher than the absorption at 320 nm. So MT4 was not likely an alcoholic

ether at C10, but an acyl ester at C30, in other words, it was 10-hydroxylgambogic acid-30-*O*-glucuronide.

4. Conclusion

In this paper, LC–ESI-MS and LC–^{1}H NMR data were analyzed to elucidate the structures of GBA metabolites in rat bile. We show that four of the metabolites of GBA were the oxides of the double bond of GBA and their glucuronide conjugates. On the basis of these metabolic profiles, we propose that GBA is metabolized as shown in Fig. 2. GBA was first oxidized by oxidase *in vivo*, and then conjugated with glucuronide.

There are several olefinic bonds in the structure of GBA. The 9,10-olefinic bond was more likely to be oxidized than the others because it was not only in a α,β-unsaturated ketone system, but also in a rigid bridged ring system. Oxidation of this bond is favorable for relieving tension.

A disadvantage of this stop-flow HPLC–NMR method was the relatively poor sensitivity, we were not able to record the NMR spectra of MT3 and MT4. To further increase the sensitivity of the method, stronger magnets or a cryoprobe could be applied in the system; prior enrichment of MT3 and MT4 by preparative HPLC could also increase the amount of MT3 and MT4 in the samples injected. An alternative for increasing sensitivity on existing LC–NMR systems is an on-line SPE add-on. It made multiple trapping of a given peak on a given SPE cartridge possible, the cartridge is then dried under nitrogen and the contents are finally eluted from the cartridge into the NMR flow probe. An additional advantage of this system is that after drying the cartridge, analytes can be measured in fully deuterated solvents and HPLC solvents do not need to deuterated, shimming is trivial and solvent suppression is mostly not required, the signals in the higher-field region would be legible. Two-dimensional proton NMR data (TOCSY and COSY) could be collected in some cases [12,13].

References

[1] B.R. Chen, Acta Acad. Med. Jiangxi 2 (1980) 1.
[2] Q.L. Guo, Q.D. You, Z.Q. Wu, S.T. Yuan, L. Zhao, Acta Pharmacol. Sin. 25 (2004) 769.
[3] Z.Q. Wu, Q.L. Guo, Q.D. You, L. Zhao, H.Y. Gu, Biol. Pharm. Bull. 27 (2004) 1769.
[4] L. Zhao, Q.L. Guo, Q.D. You, Z.Q. Wu, H.Y. Gu, Biol. Pharm. Bull. 27 (2004) 998.
[5] S. Kasibnatla, K.A. Jessen, S. Maliartchouk, J.Y. Wang, N.M. English, J. Drewe, Cell Biol. 102 (2005) 12095.
[6] K. Hao, X.Q. Liu, G.J. Wang, J. Chin. Pharm. Univ. 36 (4) (2005) 338.
[7] Y.T. Liu, K. Hao, X.Q. Liu, G.J. Wang, Acta Pharmacol. Sin. 27 (2006) 1253.
[8] R.M. Silverstein, F.X. Webster, D.J. Kiemle, Spectrometric Identification of Organic Compounds, 7th ed., John Wiley & Sons Publishing, Hoboken, 2005.
[9] S.X. Cai, H.Z. Zhang, Y. Wang, B. Tseng, K. Shailaja, D. John A, Invent Patent WO2000US02332 20000201.
[10] F. Feng, W.Y. Liu, Y.S. Chen, Q.L. Guo, Q.D. You, J. Asian Nat. Prod. Res. 9 (8) (2007) 735.
[11] J. Asano, K. Chiba, M. Tada, T. Yoshi, Phytochemistry 41 (3) (1996) 815.
[12] O. Corcoran, M. Spraul, Drug Discov. Today 8 (14) (2003) 624.
[13] A. Pukalskas, T.A. van Beek, P. de Waard, J. Chromatogr. A 1074 (2005) 81.